Multiple observations of cavitation cluster dynamics close to an ultrasonic horn tip

Peter R. Birkin,[a] Douglas G. Offin, and Christopher J. B. Vian
School of Chemistry, University of Southampton, Southampton, SO17 1BJ, United Kingdom

Timothy G. Leighton
Institute of Sound and Vibration Research, University of Southampton, Southampton, SO17 1BJ, United Kingdom

(Received 21 January 2011; revised 3 August 2011; accepted 9 September 2011)

Bubble dynamics in water close to the tip of an ultrasonic horn (~23 kHz, 3 mm diameter) have been studied using electrochemistry, luminescence, acoustics, light scattering, and high-speed imaging. It is found that, under the conditions employed, a large bubble cluster (~1.5 mm radius) exists at the tip of the horn. This cluster collapses periodically every three to four cycles of the fundamental frequency of the horn. Following the collapse of the cluster, a short-lived cloud of small bubbles (each tens of microns in diameter) was observed in the solution. Large amplitude pressure emissions are also recorded, which correlate temporally with the cluster collapse. Bursts of surface erosion (measured in real time using an electrochemical technique) and multibubble sonoluminescence emission both also occur at a subharmonic of the fundamental frequency of the horn and are temporally correlated with the bubble cluster collapse and the associated pressure wave emission.
 [DOI: 10.1121/1.3650536]

PACS number(s): 43.35.Ei, 43.35.Ty, 43.25.Yw, 43.35.Hl [AJS] Pages: 3379–3388

I. INTRODUCTION

The ultrasonic horn is one of the most common commercial ultrasonic devices, and yet its mode of operation is surprisingly complex. Through the application of an approximately sinusoidal continuous-wave (or sometimes tone-burst) voltage (of center frequency f_0 usually in the region of 20–30 kHz) to the piezoelectric stack in the shaft of the horn, the tip of the horn undergoes an approximately sinusoidal oscillation of a few tens of microns at f_0. The tip being immersed in a liquid, and the wavelength in the liquid at f_0 being much larger than the tip diameter, the direct sound field amplitude falls off rapidly with distance from the tip (as a dipole if the tip is only shallow, and as a monopole if it is very deep, which is rare). Even in the absence of cavitation, the overall sound field in the liquid itself is a combination of this direct field and that generated by the reverberation and reflections from walls of the vessel which contain the liquid.[1,2] When cavitation is modeled in this environment, the vast majority of simulations assume a single bubble in an infinite body of liquid driven by a sound field at f_0. If the driving pressure fluctuations are great enough to exceed the Blake threshold (usually around atmospheric pressure at these frequencies under normal conditions in water), microscopic pre-existing bubbles within the liquid can expand rapidly in the rarefaction portion of a sound wave. If this expansion is sufficiently large, the subsequent bubble collapse is dominated by inertial forces within the liquid and has been termed "inertial cavitation" (also known as "transient cavitation").[3,4] In contrast, during "non-inertial cavitation" the collapse is dominated by the pressure within the gas phase of the bubble interior.[5–7] The fate of a particular bubble is determined by the local conditions of frequency, pressure amplitude, solution parameters,[3,8] and its initial size, and these define the threshold conditions for generating inertial cavitation. The most common usage of ultrasonic horns is for them to generate 20–30 kHz continuous-wave fields into water or aqueous solution that has undergone no special treatment (such as degassing, deionizing) under atmospheric pressure. For such conditions the threshold acoustic pressure to generate inertial cavitation is around ~100–120 kPa (zero-to-peak amplitude), and as the driving pressure exceeds this, a relatively broad range of initial bubble sizes (from microns to tens of microns radius) will generate inertial cavitation.[9] However, this familiar scheme of single bubble dynamics has only limited applicability to a complex, though common, cavitation environment such as the horn produces, and attention must also be paid to the interactions between bubbles, and the roles of the bubbles whose size and location place them below the threshold for inertial cavitation. The distinction between inertial and non-inertial events is vital when interpreting results of sonochemical/sonoelectrochemical experiments, as many of the phenomenological effects associated with sonication occur during inertial bubble collapses.[10] Examples of inertial cavitation effects include local hot spots,[11–13] light emission,[14–16] radical generation,[17–19] shock waves,[20,21] and material erosion[22–24] or production.[25] These effects are potentially useful within a chemical environment where, for example, the processing[26] of materials or the destruction of organic pollutants is desired.[27–29] However, non-inertial cavitation can affect inertial cavitation in many ways, e.g., by shielding the sound field, setting up microstreaming currents that affect the transport of bubble nuclei and dissolved gases, etc.[30,31] In addition, solution constituents, e.g., surfactants, have been shown to influence the phenomena observed.[32,33] In order to assess the

[a]Author to whom correspondence should be addressed. Electronic mail: prb2@soton.ac.uk

activity in such multibubble cavitation fields, because of the pressure dependence in the fate of cavitation bubbles, the first consideration should be to the shape and characteristics of the sound field generated by the sound source.[1] For an ultrasonic horn, the direct field falls off dramatically with distance, such that with increasing ranges its contribution compared to the reverberant and scattered fields reduces. Normally, therefore, as the distance from the surface of the sound source is increased, there will be a point at which inertial cavitation ceases to exist and only non-inertial bubble oscillation occurs. However, this simple model is complicated by the interacting dynamics of bubbles in clouds[34] or clusters,[23,35,36] and the fact that the pressure (and flow) fields that drive those bubble dynamics can contain important contributions in addition to the emitted field that would be modeled from the horn, or measured from the horn in bubble-free conditions. Figure 1 demonstrates an example where higher frequency bubble-generated acoustic waves are important in demarcating the extent of the zone close to the horn where inertial cavitation can occur.[9,21] Figures 1(a)–1(e) show how the high frequency components are effectively scattered off of the electrode support and contribute significantly to the multibubble sonoluminescence (MBSL) spatial distribution of the system [see Fig. 1(e), for example]. The presence of such higher frequency components in the pressure field is clear in Fig. 1(f) when a hydrophone was placed within the sound field. In addition, when the horn was operated in identical conditions, except that the water used in Fig. 1(f) was replaced in Fig. 1(g) by castor oil, the measured pressure field in this case resembled the sinusoidal voltage signal supplied to the horn, and it lacked the pressure spikes caused by cavitation. The overall cavitational activity is therefore dependent on the cavitation cloud dynamics, and on components in the pressure field other than the direct radiation from the source.[21,37] Furthermore, changes in the drive conditions (e.g., amplitude) can change the effects of the cloud (e.g., in scattering, shielding, absorbing, or enhancing the sound field), such that the observables (such as the location of luminescence) can in turn change.[15,38]

Cavitation is complex enough to generate many effects and to cause difficulties when attempts are made to quantify it. Quantification of cavitation is therefore actually the quantification of the effects of cavitation. In addition, this quantification process is most safely done by the monitoring of numerous effects and comparing the results. Some common methods of quantification of the effects of cavitation (such as sonochemical yield or erosive mass loss) afford poor spatial and temporal resolution. Measurements that afford fine spatial resolution in conjunction with the correlation of time resolved measures of cavitation[39–41] provide a particularly useful approach to probing such complex cavitation environments, particularly when those measurements can be made simultaneously.

This paper reports the results from a unique combination of time resolved techniques, which are used to characterize the dynamics of cavitation induced close to the tip of an ultrasonic horn that generated the features in Fig. 1. The techniques used are electrochemical detection of surface erosion, time resolved MBSL, laser scattering, acoustic pressure measurements, and high-speed imaging. By combining these techniques it has been possible to gain insight into the dynamics of the bubble population and partially elucidate mechanisms associated with the phenomenological effects associated with inertial cavitation.

II. EXPERIMENTAL

A. The driving conditions

A commercial ultrasonic horn (Adaptive Biosystems, Luton, UK) fitted with a 3 mm diameter titanium tip was driven by a continuous sinusoidal signal from a function generator (Grundig Digimess FG 100, Derby, UK) via a power amplifier (Brüel & Kjær Type 2713, Nærum, Denmark). The function generator was interfaced with a personal computer using software written in-house, allowing the frequency, power, and duration of the ultrasound to be controlled. The nominal frequency and reference intensity (measured using a calorific technique[42]) of the horn field were $\sim$23 kHz and $\sim$50 W cm^{-2} (more precise measurements are included in each relevant figure caption).

B. Acoustoelectrochemical experiments

Acoustoelectrochemistry is the process by which mass flux,[43–45] reaction,[46,47] or erosion[48] resulting from acoustically induced liquid motion (usually bubble-generated motion[49]) are monitored by their effects on an electrochemical current, as sensed at an electrode. The detection of mass flux is sensed because, in stagnant fluid, the electrochemical current is limited by diffusion alone, and over time the region of liquid close to the electrode tip becomes depleted of active species. Liquid motion disrupts this depletion layer by introducing convection to the system.[49,50] This is sensed as an enhancement of electrochemical current. The working electrode (or sensing element) is usually made of some noble metal (such as platinum) imbedded in an insulator (such as glass or epoxy resin). In contrast, the electrodes used to sense erosion are made of a passive metal (such as lead in sulphate media[9,48] or aluminum[51]). Erosion is sensed through the current required to regrow a passivating layer that has been mechanically removed from the surface of the electrode. These sensors can have resolutions better than 100 μm and 100 μs (depending on the mechanism investigated). In this paper the investigation of the erosion technique is reported in relation to the temporal dynamics of the events generated. Figure 2 shows a schematic representation of the electrochemical rig employed. The working electrode was inserted in the bottom of the electrochemical cell, which itself was placed on an *XY* stage (Photon Control, Cambridge, UK). The stage allowed 25 mm of movement in each direction with 0.01 mm resolution, enabling the position of the working electrode to be accurately controlled in a plane below the tip of the ultrasonic horn. The position of the horn was fixed in the *XY* plane but controlled in the *Z* direction by means of a micrometer and stage (Newport, Irvine, CA), which allowed 25 mm of movement with 0.02 mm resolution. This allowed the separation between the surface of the working electrode and the tip of the ultrasonic horn to be controlled with the necessary high degree of precision.

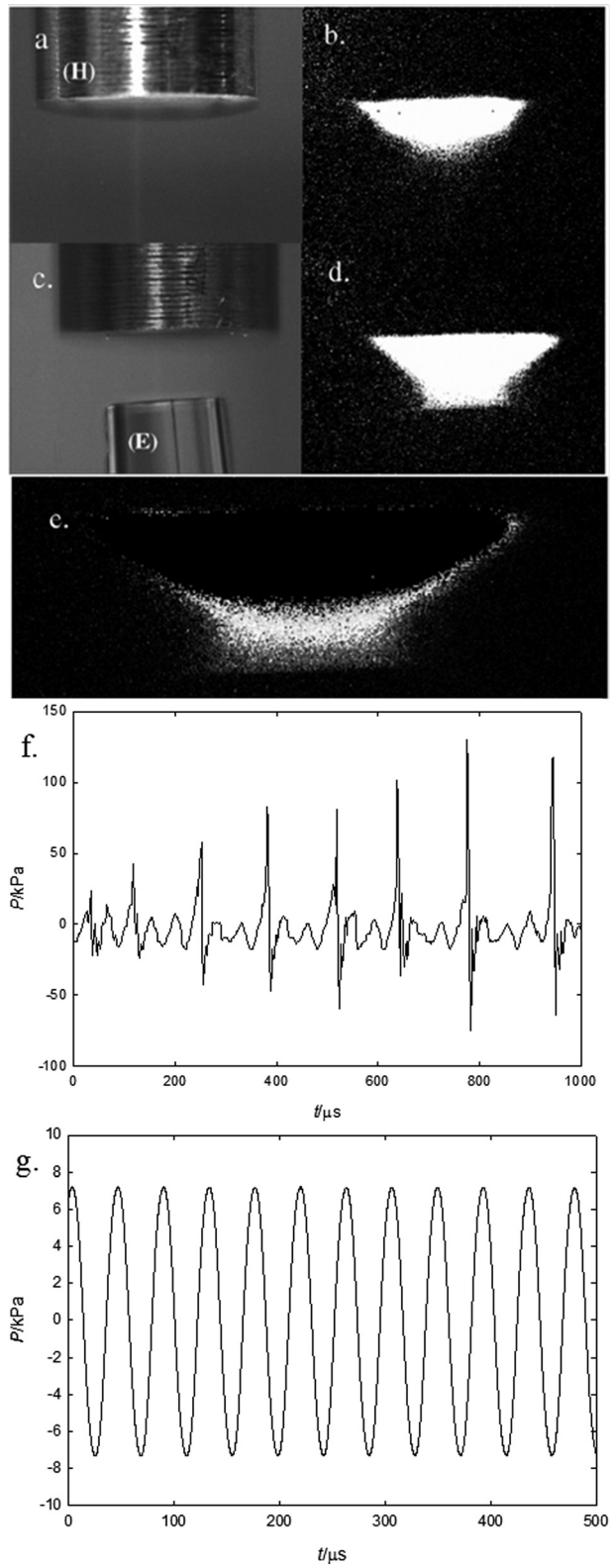

FIG. 1. A 3 mm diameter ultrasonic horn (H) is photographed in daylight without (a), then with (c), an erosion sensor placed under it (the sensor, labeled E, consists of a 25 μm diameter stainless steel vertical wire embedded in a glass tube). (b),(d) The light emission (10 min exposures) from cavitation without (b) and with (d) the erosion sensor in place, for continuous ultrasonic irradiation (22.83 kHz, nominal faceplate intensity 56 ± 5 W cm^{-2}, ~30 kPa zero-to-peak pressure amplitude at 4.5 mm below the horn). Subtraction of (c) from (d) leaves a light remnant (e), indicating that scattering of the acoustic field from the electrochemical sensor is increasing the acoustic pressure in the liquid sufficient to cause inertial cavitation at ranges from the sound source where, without such scattering, the amplitude is insufficient to generate inertial cavitation. The scattered fields generating this effect are not the direct field produced by the horn (which has a wavelength much larger than the sensor), but instead the higher frequency components generated by the cavitation generated. Experiment undertaken in 0.75 M Na_2SO_4 at 25 °C in aerobic solutions (Ref. 21). (f) The acoustic pressure (P) time history recorded below an ultrasonic horn using a calibrated hydrophone in a water tank above the inertial cavitation threshold. The distance between the tip of the ultrasonic source and the acoustic center of the hydrophone was 8.8 mm. (g) Plot of the acoustic pressure (P) time signal recorded in castor oil in a 5 dm^3 beaker. The distance between the active element of the hydrophone and the source was 4.8 mm (see Ref. 9 for further details).

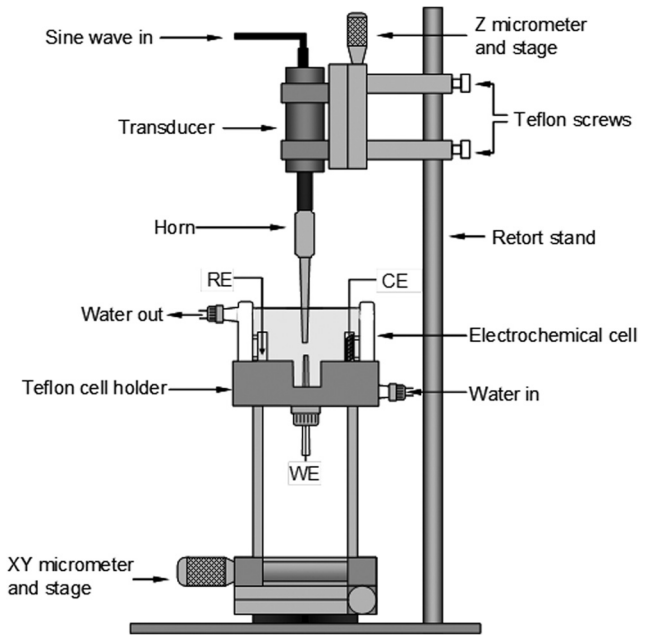

FIG. 2. Illustration of the acoustoelectrochemical setup employed to record the electrochemical response of the working electrode (WE) as a function of position with respect to the sound source. Note CE and RE refer to the counter and reference electrode, respectively.

C. Acoustic measurements

All acoustic pressures were measured with a Brüel & Kjær type 8103 hydrophone and Brüel & Kjær type 2635 charge amplifier. The data were recorded by means of an oscilloscope (Le Croy 9310 AM, Chestnut Ridge, NY, or Tektronix TDS 220, Beaverton, OR). Whilst the type 8103 is a relatively small hydrophone, the active element (a cylinder measuring 6 mm × 6 mm)[52] is still large compared to the pressure gradients expected. Consideration of this in terms of spatial averaging effects is paramount when recording and interpreting pressure measurements. However, the element is small enough to satisfy the condition that the dimensions are less than one-tenth of the wavelength of the driving sound wave used in this work (~7 cm), which implies that the hydrophone is omnidirectional with respect to the driving (~23 kHz) pressure wave. However, for frequencies above 180 kHz these hydrophones are known to be limited, with loss in sensitivity, and their phase response is rarely calibrated. Hence, measurements of shock pressure amplitudes will be underestimated under these conditions.

D. Luminescence experiments

The temporal characteristics of MBSL were investigated using an (EMI-Gencon Inc. RFI/B-293, Plainview, NY) photomultiplier tube (PMT) powered by 2 kV power supply (Brandenburg 475R, Worthing, UK). The PMT was fixed to the underside of a wooden platform, which had a hole (10.5 cm diameter) in the center. A sliding cover allowed the hole to be covered when not in use. The cell, which was a Pyrex™ crystallization dish (internal diameter, 93 mm depth, 50 mm), was placed above the PMT and the horn was positioned such that the tip was 15 mm below the surface of the solution (0.75 mol dm^{-3} Na_2SO_4) and directly above the PMT. In order to measure the pressure and light output simultaneously, a hydrophone was placed in the cell such that the acoustic center was at a lateral distance of 15 mm from the center of the tip of the horn. An oscilloscope (Tektronix TDS 224) was used to record the output from the PMT and the hydrophone simultaneously, allowing the pressure signal and light output to be temporally correlated.

E. High-speed imaging

High-speed video footage was recorded using a (Photosonics Phantom V7, Burbank, CA, or Photron APX RS, San Diego, CA) [both capable of frame rates exceeding 100 000 frames per second (fps)] digital video camera fitted with a monozoom lens. It was necessary to backlight the subject so that the horn and bubbles appear as silhouettes. For high-speed imaging experiments a cylindrical glass cell (75 mm internal diameter, 105 mm height) fitted with a flat window was used.

F. Laser scattering experiments

For laser scattering experiments a 3 dm^3 beaker was modified by the scientific glass blowing service in the School of Chemistry at the University of Southampton to increase the height and volume to 3.5 dm^3, and include optically flat windows (4 cm diameter) on opposite sides of the beaker. Also included was a hollow glass support, which was terminated with an SQ 13 fitting, allowing a hydrophone to be positioned in the center of the beaker at a height of 12 cm from the base. The overall height of the beaker was 23 cm and the internal radius was 7 cm. The beaker was filled to a height of 19 cm with pure water and the ultrasonic horn was positioned such that it was in the center of the beaker submerged to a depth of 15 mm. A laser (UG 5001-21 diode laser, 1 mW, 635 nm, RS) was shone through the beaker and detected by means of a photodiode (AEPX65, RS) and an amplifier circuit made in-house.[53] The photodiode had an active area of 0.8 mm^2. The electronics were such that the maximum output (under direct illumination by the laser) was −1.2 V. Any scattering of the beam resulted in an increase in the output voltage (i.e., the voltage became less negative). Prior to each experiment, the position of the photodiode was adjusted by means of an *XYZ* stage (Newport, 0.02 mm resolution) such that the output was at a maximum negative value. The laser beam was flat with a width of 3 mm and was orientated such that it was parallel with the face of the ultrasonic horn. The distance between the horn and the beam was determined by lowering the horn (by means of a micrometer and stage) until it just blocked the beam and then retracting the horn a known distance. In all cases the distance used was 1.4 mm. The pressure and photodiode output were recorded using a Le Croy 9310 AM oscilloscope. For experiments where the distance between the horn and the hydrophone was varied, the glass support was blanked off and the hydrophone was clamped in place using a retort stand.

G. Chemicals and solutions

All solutions were made up using water from an (USF Elga Purelab Option E10, Marlow, UK) water purification system. Water purified in this manner had a conductivity of

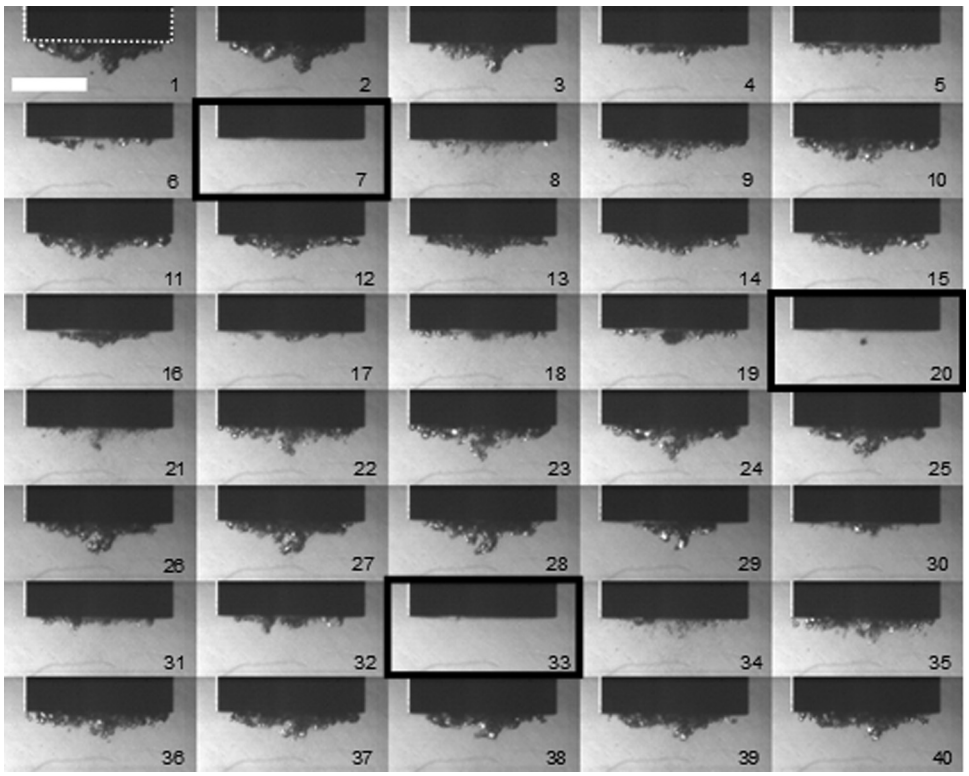

FIG. 3. Image showing 40 consecutive frames taken at 100 000 fps showing the tip of an ultrasonic horn (dark oblong at the top of each frame) operating at 22.85 kHz. The scale bar in frame 1 represents 1.5 mm and the white dotted outline shows the solid/liquid boundary of the piston like emitter. The dark outlines show frames (see frames 7, 20, and 33) where the solution is apparently clear. The cell contained aerobic aqueous media at 18 °C–23 °C.

below 0.1 μS cm^{-1} and a low organic content (manufacture quoted TOC <30 ppb). Na_2SO_4 (BDH, AnalaR) was used as received.

III. RESULTS AND DISCUSSION

A. High-speed imaging and laser scattering

In order to study the dynamics of the bubble population, first high-speed imaging was employed. Figure 3 shows a set of images recorded using a high-speed camera of the region below the operating ultrasonic horn. Here the tip of the sound source is seen in the upper center of each image. The framing rate (100 000 fps) is high enough to resolve the growth and collapse of a cluster of bubbles located on the tip of the sound source. Interestingly, this bubble cloud appears to grow and collapse periodically (with a period close to 130 μs). However, the period of this motion does not match the period of the oscillation of the ultrasonic probe's tip (in this case ~43 μs or a frequency of ~23 kHz). Rather, Fig. 3 shows that the collapse process occurs over ~130 μs or three sound cycle periods. This can be seen as the 13 frame interlude between complete clearing of the cluster of bubbles from the tip (see highlighted frames 7, 20, and 33). The repetitive nature of these events at 1/3 the fundamental frequency match the periodic shock wave like emission in the acoustic output of the system, which has been reported previously (see Fig. 1 and Ref. 9). Note that in the absence of cavitation [e.g., by suppressing this process using castor oil instead of water—see Fig. 1(g)] the pressure wave became sinusoidal in nature.[9] This indicates that the shock wave like emission is strongly linked to the cavitation process within the water rather than being an intrinsic property of the transducer.

The periodic nature of the bubble events recorded using this high-speed camera technique was investigated further using a laser scattering technique. Here the beam of a diode laser was passed through the solution at a defined distance below the tip of the operating ultrasonic horn. A photodiode was then used to detect the intensity of the beam. In the absence of any scattering objects in the laser beam's path (e.g., bubbles) the voltage signal recorded from the photodiode is at its most negative. However, scattering due to bubbles or other objects is seen as a reduction in the negative voltage

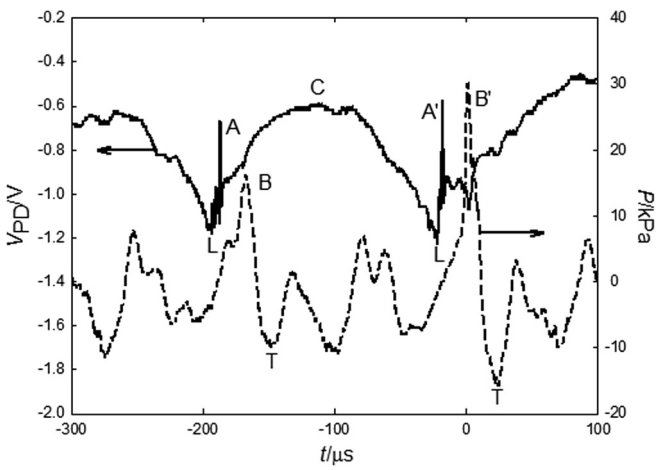

FIG. 4. Plot showing the acoustic pressure (P) (– –) and output from a photodiode (V_{PD}) (—) recorded simultaneously under exposure to ultrasound (23.10 kHz). The photodiode was aligned with a laser beam, which was passing below the tip of the horn at a distance of 1.4 mm. The distance between the horn and the hydrophone was 20 ± 1 mm. The cell contained aerobic purified water at 18 °C–23 °C.

(towards zero when the laser beam is totally obscured) recorded by the photodiode. Figure 4 shows a typical signal obtained from the photodiode as a function of time during operation of the ultrasonic horn. In this experiment, a hydrophone was also placed in the cell to record simultaneously the acoustic pressure amplitude as a function of time. Initially the value of V_{PD} is -0.7 V. This indicates that there is some scattering of the laser beam. The value of V_{PD} is then seen to decrease, reaching a minimum value of approximately -1.2 V, corresponding to clear passage of the laser beam through the solution below the tip of the probe. This is ascribed to the absence of a cluster of large, visible cavitation bubbles, such as the situation shown in Fig. 3, frames 7, 20, and 33. Interestingly, this solution clearing is almost immediately followed (i.e., within 10 μs) by a sharp rise or spike in the photodiode signal (labeled A). The output then increases to the original value (labeled C) before this cycle of decrease, spike (A′) and increase is repeated. The period of these events is $\sim$170 μs (or four cycles of the ultrasonic wave employed). The events (labeled A and A′) correspond to the situation when the laser was blocked by an object, presumably a bubble or bubble cloud. At the same time, the hydrophone data give an insight into the origin of the effects observed with the laser scattering experiment. About 19 μs after each event of periodic clearing and sudden spike in the laser signal (labeled A and A′) there is a spike in the pressure signal (labeled B and B′). The clarity of the shock emission is obscured by the reverberant nature of the relatively small vessel ($\sim$3.5 dm^3) employed in the experiments. However, clearer evidence for this pressure wave (the exact profile of which is probably not captured by the hydrophone because of the latter's amplitude and phase response at high frequencies) has been reported previously in a larger vessel ($\sim$2 m^3) with the hydrophone placed closer to the tip of the sound source (see Fig. 1 and Ref. 9). The link between these events and the hydrophone data can be further highlighted by varying the distance between the tip of the ultrasonic probe and the hydrophone and then measuring the delay between the events in the laser scattering experiment and the hydrophone data. The results of such an experiment are shown in Fig. 5, which was performed in the 3.5 dm^3 vessel. Here, the time between the pressure pulse (B) and the spikes in the scattering signal (A) can be seen to increase as the distance between the hydrophone and the tip of the ultrasonic probe was increased. The relationship is linear and can be used to calculate the speed of sound in the liquid as 670 ± 100 m s^{-1}. This is much less than the speed of sound in bulk water, but this may be expected in the presence of bubbles. This

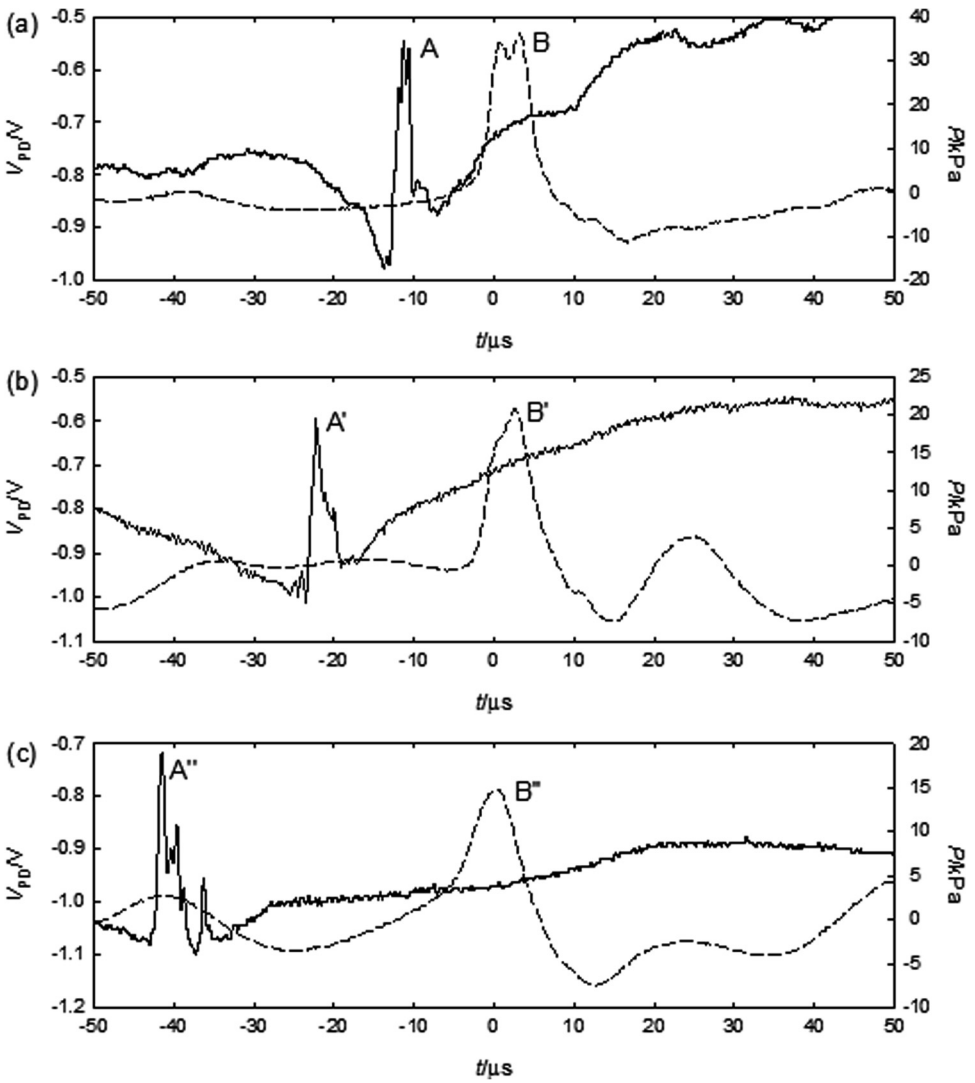

FIG. 5. Plot showing the acoustic pressure (P) (– –) and output from a photodiode (V_{PD}) (—) recorded simultaneously under exposure to ultrasound (22.83 kHz, nominal faceplate intensity 56 ± 5 W cm^{-2}, $\sim$30 kPa zero-to-peak pressure amplitude at 4.5 mm below the horn) at three horn-to-hydrophone distances (a) 14.2 mm, (b) 28.2 mm, and (c) 52.2 mm. The cell contained aerobic purified water at 18 °C–23 °C.

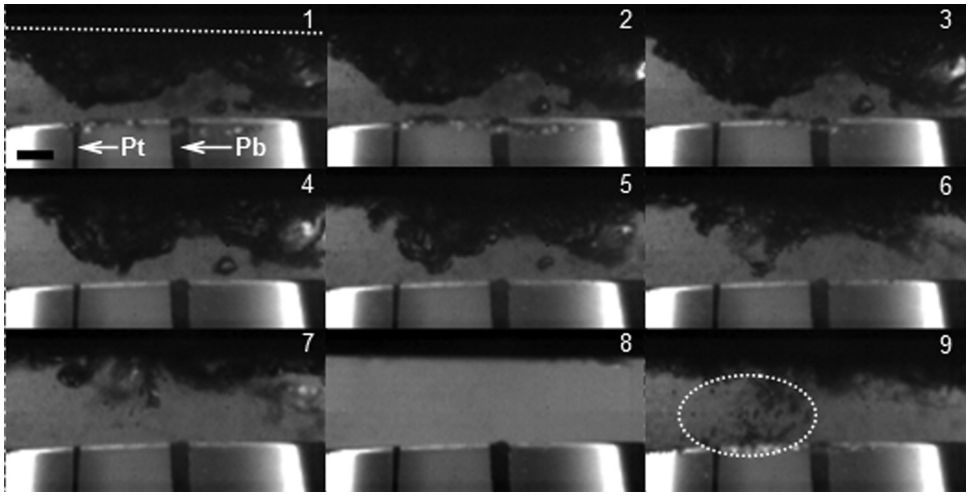

FIG. 6. Nine frames taken from high-speed video footage recorded at 100 000 fps of the tip of the horn and an electrode during exposure to ultrasound (22.83 kHz, nominal faceplate intensity 56 ± 5 W cm^{-2}, ~30 kPa zero-to-peak pressure amplitude at 4.5 mm below the horn). The tip of the horn is at the top of each frame (shown by the dotted line in frame 1). A dual electrode containing a Pb (125 μm diameter) and a Pt (50 μm diameter) wire (labeled in frame 1) can be seen in the bottom of each frame. The scale bar in the bottom left corner of frame 1 represents 250 μm.

retardation of sound velocity in bubbly liquids is well known,[54] and similar values have been measured in vessels in which inertial cavitation has been generated.[1]

While the high-speed imaging shown in Fig. 3 can capture the periodic collapse of a large bubble cloud at the tip of the ultrasonic horn, there is nothing visible to explain the transient laser scattering observed (the spikes labeled A and A′ in Fig. 4). However, further high-speed imaging experiments have revealed evidence of transient bubble clouds. Figure 6 shows a sequence of frames collected at 100 000 fps below an operating ultrasonic horn and above an electrode. The collapse of the cluster formed below the ultrasonic tip can be seen between frames 1 and 7. Frame 8 is almost totally clear. This is consistent with the data presented thus far. However, frame 9 shows a group of small bubbles in the bulk solution (highlighted by the dotted oval). They are also much smaller than the large cluster that exists at the tip of the horn. Such bubbles have been detected in other scenarios,[40] in response to a search for the cause of spikes in sonoluminescence emission.[41] It is proposed that these events are partially responsible for the spike in the laser scattering data (note the shock itself may give a perturbation of the laser through Schlieren effects[55]). A further example of these transient clouds of bubbles is shown in Fig. 7. Figure 7 shows a set of images, which depict key stages of the bubble population dynamics observed and described earlier, imaged by illumination through the cell to the camera (creating a shadow effect that is useful in imaging bubbles produced within the media). Figure 7(a) shows the cluster at the tip of the horn (labeled BC) and a thinner cloud of bubbles (labeled BN) below the cluster. Figures 7(a)–7(c) show the bubble cluster collapsing. In Fig. 7(d), both the bubble cluster on the tip of the horn and the bubble cloud (BN) are no longer visible in the image. Figure 7(e) shows a transient bubble cloud highlighted in a dotted oval. Both the bubble cluster and the thinner bubble cloud are reformed after the transient bubble cloud event [see Figs. 7(f)–7(h)]. This agrees with the laser scattering data shown in Fig. 4. However, the images also clearly show that the preexisting bubbles [see Fig. 7(a), BN] are compressed before a "rebound" event was observed [see Fig. 7(d)].

B. Correlation of bubble dynamics with physical effects

The correlation of these dynamics with the observed effects of cavitation was investigated by first measuring the

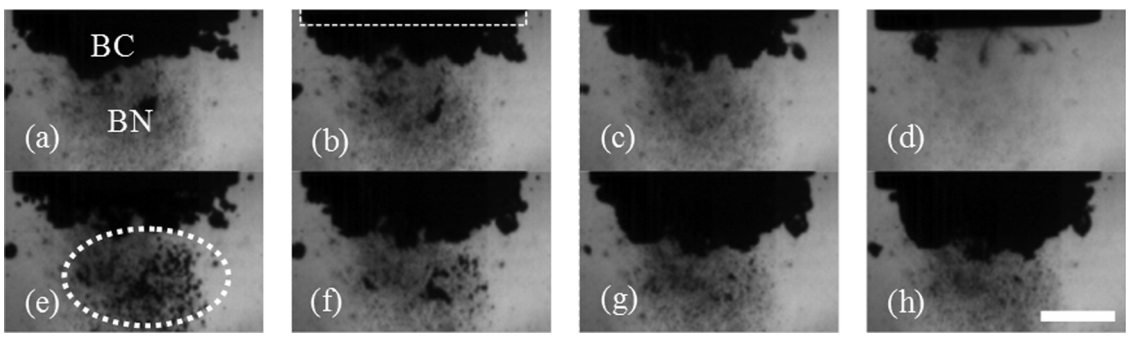

FIG. 7. Consecutive frames from high-speed imaging showing a side-on view of the cavity collapse sequence and zones of cavitation events. (a) The large cavity (labeled BC) on the tip of the piston like emitter [border highlighted by dotted line in (b)]. Also shown in (a) is a cloud of smaller unresolved bubbles (labeled BN) below the large cluster. (d) The disappearance of the cavity cluster (BC) and bubble cloud (BN) in response to the pressure emissions generated. (e) The transient cloud (highlighted with a dotted oval) formed after the disappearance of the cluster. (f)–(h) The system has returned to the initial state (e.g., a bubble cluster and cloud). Note the scale bar in (h) represents 1 mm. The frame rate was 105 000 fps with an exposure time of 2 μs. The cell contained aerobic purified water at 22 °C ± 1 °C. Image taken using transmission of light through the cell (hence the shadow effect observed to highlight bubble cluster) to a Photron APX-RS camera. See Ref. 56 for an example of a movie sequence illustrating the cluster collapse and transient bubble cloud.

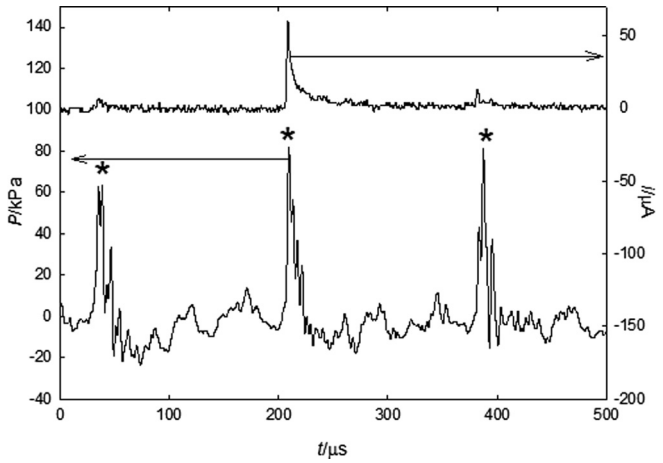

FIG. 8. Acoustic pressure (P) and current (i) recorded at a passivated lead electrode (125 μm diameter) held at +0.8 V vs saturated calomel electrode in a solution of 0.75 M Na_2SO_4 under exposure to ultrasound (23.10 kHz, nominal faceplate intensity 56 ± 5 W cm^{-2}). The electrode-to-horn distance was 1 mm and the horn-to-hydrophone distance was 10 ± 1 mm. The experiment was performed under aerobic conditions in a cylindrical cell (45 mm diameter, 45 mm depth) at 25 °C ± 1 °C. Note that the asterisks (*) refer to the shock waves emitted by the cavity collapse process.

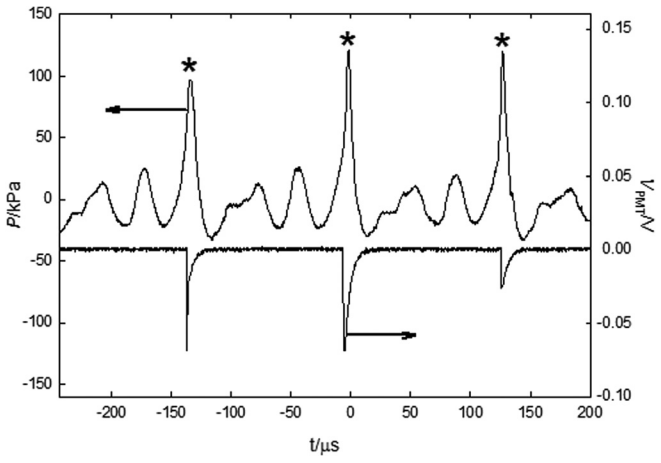

FIG. 9. Plot showing the acoustic pressure (P, upper trace) and output from the PMT (V_{PMT}, lower trace) as a function of time under exposure to ultrasound (23.10 kHz, nominal faceplate intensity 56 ± 5 W cm^{-2}). The horn-to-hydrophone distance was 15 ± 1 mm. The experiment was performed under aerobic conditions in a cylindrical cell (93 mm diameter, 50 mm depth). The cell contained aerobic aqueous 0.75 M Na_2SO_4 at 18 °C–23 °C. Note that the asterisks (*) refer to the shock waves emitted by the cavity collapse process.

response of a surface erosion sensitive electrode[48,57] (in this case a passivated Pb electrode) within this environment. Figure 8 shows the current time transient recorded for such an electrode in conjunction with the acoustic pressure signal recorded simultaneously with a hydrophone. Note that the lower trace shows the acoustic pressure trace, which is somewhat distorted because these data were recorded in a relatively small cylindrical cell (volume 71.5 cm^3). As a result, the hydrophone was subject to reverberant field effects in addition to the direct field and signals associated with cavitation activity. Nevertheless, pressure spikes [labeled by an asterisk (*)] can be seen to occur periodically, in a similar fashion to those shown previously. The upper trace shows the current recorded at the same time. The electrode was positioned 1 mm from the tip of the horn and the hydrophone was 10 ± 1 mm from the tip of the horn. In order to correlate the current and pressure data, 15 μs has been added to the current time trace. This is to account for the delay caused by the finite speed of sound in the liquid. However, owing to uncertainties in the speed of sound (as a result of the unknown bubble population) and the location of the hydrophone, there is an error of at least ± 4 μs. Nevertheless, a repassivation current time transient can be seen to occur at time $t \sim 210$ μs, which correlates temporally with a pressure spike. A second, much smaller transient can be seen at time $t \sim 380$ μs (four pressure cycles later), which also correlates with a large pressure spike. While it must be noted that the timing of the pressure spike is by no means exact, it is clear that the erosion of the electrode appears to be associated with the shock wave event. In addition to these erosion data and temporally correlated pressure and laser scattering shown above, MBSL data were also recorded. Figure 9 shows the MBSL output recorded by means of a PMT and the corresponding acoustic pressure time history. Again, light output (negative voltage spikes) correlates temporally with the high pressure spikes and occurs at $1/3$ of the fundamental frequency of the horn. This suggests that MBSL is also associated with the events that occur at the time of the subharmonic pressure spike emission. It is interesting to note that, in the case of MBSL, for every subharmonic pressure spike seen in the hydrophone signal there is corresponding light output. In contrast, not every shock wave seen in Fig. 8 leads to a repassivation transient. This suggests that although a global shock wave is generated, which can be detected by the hydrophone, it is the action of a localized event (possible microjetting) that leads to surface erosion. The lead microelectrode represents a small target, whereas the PMT collects light from a wide area. Hence only events that occur in a suitable location will be detected by the passivated electrode.

C. The mechanism

The evidence presented thus far suggests that the environment below an operating ultrasonic horn is very complex indeed. Clearly, shock waves, bursts of bubble events, erosion, and MBSL emission all occur in a local space and within a short time window. It is interesting to discuss the possible mechanisms responsible for these physical observations. The high-speed imaging shows that a cluster collapse[23,35,36] is produced on the surface of the operating ultrasonic horn. This cluster collapse correlates with the extended periodicity of the other experimental observations (e.g., in this case the erosion, shock, and MBSL measurements occur on every third or fourth cycle of the ultrasonic wave in time with the laser scattering and high-speed imaging of the cluster collapse). However, the actual mechanisms responsible for surface erosion and MBSL are less clear. The laser scattering and high-speed imaging suggests that after the large gas cavity on the surface of the horn has collapsed, a cloud of small transient bubbles is observed. These are at an extended distance compared to the cavity collapse itself,

which is estimated to extend ~1400 μm from the surface of the horn. As erosion and MBSL have been observed at greater distances than this,[9,21] one could suggest that these small, transient bubble events are responsible for both effects, or that the transient bubble cloud marks the passage of a pressure wave through the liquid, and the arrival of that pressure wave on, say, the erosion sensor generates further cavitation and thence erosion. It is useful at this point to discuss the sequence of events that could be responsible for these experimental observations.

Inertial collapse of an individual bubble can generate a positive pressure pulse, which, close to the bubble, can have an amplitude very much greater than that of the wave that caused the collapse,[58] although the amplitude of this wave will, of course, decay as it propagates to the far field.[37] However, high amplitude tensile components can also be generated, for example, as these compressive waves reflect off neighboring bubbles.[37,58] Furthermore, there will be edge waves from the perimeter of the horn face, and a complex of waves generated within (and at the perimeter of) the horn material itself.[10] Hence, the collapse of a cluster against the horn face, and interaction of the pressure fields within these media, will generate a complex pressure wave that propagates outwards.

The short lived transparency of the liquid [see Fig. 7(d)] is assumed to coincide with the low laser scattering (see Fig. 4, labeled L) and is a result of compression of bubbles by the above-mentioned compressive pulse. However, the limited hydrophone response cannot capture its true form or that of the subsequent large tension (although both have been observed in the experiments, see Fig. 4, B and T, for example). Nevertheless, the action of the tension on previously compressed bubbles would be expected to produce the extreme bubble growth and subsequent high transient laser scattering observed. This conclusion is supported[59] by cavitation histories associated with shock waves, particularly during lithotripsy.[20,60,61]

It is worth noting that only surface erosion and MBSL have been investigated here. However, the consequences for chemical activity within this environment are unclear. If chemical activity is linked to MBSL output of a system, as suggested in other reports,[18,62,63] one would also expect this to follow this cluster collapse and transient bubble cloud mechanism and associated timing. Also, the discussion thus far has concentrated on the space close to the tip of the sound source where inertial events are generated (<3 mm away from the center of the piston like emitter employed here). While this region is rich in mechanistic detail, it only represents a small fraction of the total volume of the liquid. In other locations, outside of this zone, the behavior of bubbles will be non-inertial but still of interest.

IV. CONCLUSIONS

A multisensor/imaging approach to the environment below an operating ultrasonic horn has been reported. The environment has been shown to be extremely complex with shock waves, inertial cavitation, cluster collapses, and transient bubble clouds observed. These observations indicate that physical measurements such as surface erosion and MBSL emission from such an environment are strongly periodic in nature and occur at a subharmonic resonance related to the dynamics of bubble clouds within this media.

ACKNOWLEDGMENTS

We thank the EPSRC for funding (EP/E024408/1 and EP/D05849X/1) and the EPSRC Instrument Loan Pool for assistance with some of the high-speed imaging reported in this paper.

[1]P. R. Birkin, T. G. Leighton, J. F. Power, M. D. Simpson, A. M. L. Vingotte, and P. F. Joseph, "Experimental and theoretical characterisation of sonochemical cells. Part 1. Cylindrical reactors and their use to calculate the speed of sound in aqueous solutions," J. Phys. Chem. A **107**, 306–320 (2003).
[2]T. G. Leighton, P. R. White, C. L. Morfey, J. W. L. Clarke, G. J. Heald, H. A. Dumbrell, and K. R. Holland, "The effect of reverberation on the damping of bubbles," J. Acoust. Soc. Am. **112**, 1366–1376 (2002).
[3]C. K. Holland and R. E. Apfel, "An improved theory for the prediction of microcavitation thresholds," IEEE Trans. Ultrason. Ferroelectr. Freq. Control **36**, 204–208 (1989).
[4]R. E. Apfel and C. K. Holland, "Gauging the likelihood of cavitation from short-pulse, low-duty cycle diagnostic ultrasound," Ultrasound Med. Biol. **17**, 179–185 (1991).
[5]H. G. Flynn, "Cavitation dynamics: I. Free pulsations and models for cavitation bubbles," J. Acoust. Soc. Am. **58**, 1160–1170 (1975).
[6]H. G. Flynn, "Cavitation dynamics: I. A mathematical formulation," J. Acoust. Soc. Am. **57**, 1379–1396 (1975).
[7]T. G. Leighton, *The Acoustic Bubble* (Academic, London, 1994), Sec. 4.3.1, pp. 312–329.
[8]T. G. Leighton, "Bubble population phenomena in acoustic cavitation," Ultrason. Sonochem. **2**, S123–S136 (1995).
[9]P. R. Birkin, D. G. Offin, and T. G. Leighton, "Experimental and theoretical characterisation of sonochemical cells. Part 2: Cell disruptors (ultrasonic horns) and cavity cluster collapse," Phys. Chem. Chem. Phys. **7**, 530–537 (2005).
[10]T. G. Leighton, "What is ultrasound?," Prog. Biophys. Mol. Biol. **93**, 3–83 (2007).
[11]K. S. Suslick, "The chemical effects of ultrasound," Sci. Am. **260**, 80–86 (1989).
[12]K. S. Suslick, "Sonochemistry," Science **247**, 1439–1445 (1990).
[13]K. S. Suslick, D. A. Hammerton, and R. E. Cline, "The sonochemical hotspot," J. Am. Chem. Soc. **108**, 5641–5642 (1986).
[14]L. A. Crum and G. T. Reynolds, "Sonoluminescence produced by 'stable' cavitation," J. Acoust. Soc. Am. **78**, 137–139 (1985).
[15]A. J. Walton and G. T. Reynolds, "Sonoluminescence," Adv. Phys. **33**, 595–660 (1984).
[16]S. Putterman, P. G. Evans, G. Vazquez, and K. Weninger, "Cavitation science—Is there a simple theory of sonoluminescence?," Nature (London) **409**, 782–783 (2001).
[17]A. Weissler, H. W. Cooper, and S. Snyder, "Chemical effect of ultrasonic waves: Oxidation of potassium iodide solution by carbon tetrachloride," J. Am. Chem. Soc. **72**, 1769–1775 (1950).
[18]P. R. Birkin, J. F. Power, A. M. L. Vingotte, and T. G. Leighton, "A 1 kHz frequency resolution study of a variety of sonochemical processes," Phys. Chem. Chem. Phys. **5**, 4170–4174 (2003).
[19]G. Mark, A. Tauber, R. Laupert, H. P. Schuchmann, D. Schulz, A. Mues, and C. von Sonntag, "OH-radical formation by ultrasound in aqueous solution—Part II: Terephthalate and Fricke dosimetry and the influence of various conditions on sonolytic yield," Ultrason. Sonochem. **5**, 41–52 (1998).
[20]B. Wolfrum, T. Kurz, R. Mettin, and W. Lauterborn, "Shock wave induced interaction of microbubbles and boundaries," Phys. Fluids **15**, 2916–2922 (2003).
[21]P. R. Birkin, D. G. Offin, P. F. Joseph, and T. G. Leighton, "Cavitation, shock waves and the invasive nature of sonoelectrochemistry," J. Phys. Chem. B **109**, 16997–17005 (2005).
[22]F. J. Heymann, "Towards quantitative prediction of liquid impact erosion," ASTM Spec. Tech. Publ. **474**, 212–248 (1970).
[23]I. Hansson and K. A. Morch, "The dynamics of cavity clusters in ultrasonic (vibratory) cavitation erosion," J. Appl. Phys. **51**, 4651–4658 (1980).

[24]R. Garcia, F. G. Hammitt, and R. E. Nystrom, "Correlation of cavitation damage with other material and fluid properties," ASTM Spec. Tech. Publ. **408**, 239–279 (1967).
[25]K. Okitsu, M. Ashokkumar, and F. Grieser, "Sonochemical synthesis of gold nanoparticles: Effects of ultrasound frequency," J. Phys. Chem. B **109**, 20673–20675 (2005).
[26]Y. G. Adewuyi, "Sonochemistry: Environmental science and engineering applications," Ind. Eng. Chem. Res. **40**, 4681–4715 (2001).
[27]J. Berlan, F. Trabelsi, H. Delmas, A. M. Wilhelm, and J. F. Petrignani, "Oxidative degradation of phenol in aqueous media using ultrasound," Ultrason. Sonochem. **1**, S97–S102 (1994).
[28]M. R. Hoffmann, I. Hua, and R. Hoechemer, "Application of ultrasonic irradiation for the degradation of chemical contaminants in water," Ultrason. Sonochem. **3**, S163–S172 (1996).
[29]M. E. Abdelsalam and P. R. Birkin, "A study investigating the sonoelectrochemical degradation of an organic compound employing Fenton's reagent," Phys. Chem. Chem. Phys. **4**, 5340–5345 (2002).
[30]P. R. Birkin, T. G. Leighton, and Y. E. Watson, "The use of acoustoelectrochemistry to investigate rectified diffusion," Ultrason. Sonochem. **11**, 217–221 (2004).
[31]M. J. W. Pickworth, P. P. Dendy, T. G. Leighton, and A. J. Walton, "Studies of the cavitational effects of clinical ultrasound by sonoluminescence: 2. Thresholds for sonoluminescence from a therapeutic ultrasound beam and the effect of temperature and duty cycle," Phys. Med. Biol. **33**, 1249–1260 (1988).
[32]M. Ashokkumar and F. Grieser, "The effect of surface active solutes on bubbles in an acoustic field," Phys. Chem. Chem. Phys. **9**, 5631–5643 (2007).
[33]A. Brotchie, M. Ashokkumar, and F. Grieser, "Effect of water-soluble solutes on sonoluminescence under dual-frequency sonication," J. Phys. Chem. C **111**, 3066–3070 (2007).
[34]Z. Zeravcic, D. Lohse, and W. van Saarloos, "Collective oscillations in bubble clouds," J. Fluid Mech. **680**, 114–149 (2011).
[35]B. Vyas and C. M. Preece, "Stress produced in a solid by cavitation," J. Appl. Phys. **47**, 5133–5138 (1976).
[36]I. Hansson, V. Kedrinskii, and K. A. Morch, "On the dynamics of cavity clusters," J. Phys. D: Appl. Phys. **15**, 1725–1734 (1982).
[37]A. R. Jamaluddin, G. J. Ball, C. K. Turangan, and T. G. Leighton, "The collapse of single bubbles and calculation of the far-field acoustic emissions for cavitation induced by shock wave lithotripsy," J. Fluid Mech. **677**, 305–341 (2011).
[38]N. C. Eddingsaas and K. S. Suslick, "Evidence for a plasma core during multibubble sonoluminescence in sulfuric acid," J. Am. Chem. Soc. **129**, 3838–3839 (2007).
[39]C. J. B. Vian, P. R. Birkin, and T. G. Leighton, "Cluster collapse in a cylindrical cell: Correlating multibubble sonoluminescence, acoustic pressure and erosion," J. Phys. Chem. C **114**, 16416–16425 (2010).
[40]T. G. Leighton, A. J. Walton, and J. E. Field, "High-speed photography of transient excitation," Ultrasonics **27**, 370–373 (1989).
[41]T. G. Leighton, "Transient excitation of insonated bubbles," Ultrasonics **27**, 50–53 (1989).
[42]T. J. Mason, J. P. Lorimer, and D. M. Bates, "Quantifying sonochemistry—Casting some light on a black art," Ultrasonics **30**, 40–42 (1992).
[43]F. Marken, J. C. Eklund, and R. G. Compton, "Voltammetry in the presence of ultrasound," J. Electroanal. Chem. **395**, 335–339 (1995).
[44]H. H. Zhang and L. A. Coury, "Effects of high-intensity ultrasound on glassy-carbon electrodes," Anal. Chem. **65**, 1552–1558 (1993).
[45]C. R. S. Hagan and L. A. Coury, "Comparison of hydrodynamic voltammetry implemented by sonication to a rotating-disk electrode," Anal. Chem. **66**, 399–405 (1994).
[46]P. R. Birkin, J. F. Power, and T. G. Leighton, "Electrochemical evidence of $H^{\cdot}$ produced by ultrasound," J. Chem. Soc., Chem. Commun. **46**, 2230–2231 (2001).
[47]P. R. Birkin, J. F. Power, T. G. Leighton, and A. M. L. Vingotte, "Cathodic electrochemical detection of sonochemical radical products," Anal. Chem. **74**, 2584–2590 (2002).
[48]P. R. Birkin, R. O'Connor, C. Rapple, and S. Silva-Martinez, "Electrochemical measurement of erosion from individual cavitation generated from continuous ultrasound," J. Chem. Soc., Faraday Trans. **94**, 3365–3371 (1998).
[49]Y. E. Watson, P. R. Birkin, and T. G. Leighton, "Electrochemical detection of bubble oscillation," Ultrason. Sonochem. **10**, 65–69 (2003).
[50]P. R. Birkin and S. Silva-Martinez, "The effect of ultrasound on mass transfer to a microelectrode," J. Chem. Soc., Chem. Commun. **17**, 1807–1808 (1995).
[51]C. J. B. Vian, P. R. Birkin, and T. G. Leighton, "Opto-isolation of electrochemical systems in cavitation environments," Anal. Chem. **81**, 5064–5069 (2009).
[52]*Application Notes—Introduction to Underwater Acoustics* (Brüel & Kjær, Nærum Offset, Nærum, Denmark), pp. 1–27.
[53]D. G. Offin, "Acoustoelectrochemical characterisation of cavitation and its use in the study of surface processes," Ph.D. thesis, University of Southampton, 2006.
[54]F. E. Fox, S. R. Curley, and G. S. Larson, "Phase velocity and absorption measurements in water containing air bubbles," J. Acoust. Soc. Am. **27**, 537–539 (1955).
[55]J. Noack and A. Vogel, "Single-shot spatially resolved characterization of laser-induced shock waves in water," Appl. Opt. **37**, 4092–4099 (1998).
[56]See supplementary material at E-JASMAN-130–034191 for an example of high-speed imaging of the cluster collapse and the transient bubble cloud.
[57]P. R. Birkin, D. G. Offin, and T. G. Leighton, "A novel dual microelectrode for investigating mass transfer and surface erosion caused by cavitation," Electrochem. Commun. **6**, 1174–1179 (2004).
[58]C. K. Turangan, A. R. Jamaluddin, G. J. Ball, and T. G. Leighton, "Free-Lagrange simulations of the expansion and jetting collapse of air bubbles in water," J. Fluid Mech. **598**, 1–25 (2008).
[59]T. G. Leighton, F. Fedele, A. Coleman, C. McCarthy, S. Ryves, A. Hurrell, A. De Stefano, and P. R. White, "A passive acoustic device for real-time monitoring the efficacy of shockwave lithotripsy treatment," Ultrasound Med. Biol. **34**, 1651–1665 (2008).
[60]R. O. Cleveland, O. A. Sapozhnikov, M. R. Bailey, and L. A. Crum, "A dual passive cavitation detector for localized detection of lithotripsy-induced cavitation in vitro," J. Acoust. Soc. Am. **107**, 1745–1758 (2000).
[61]D. S. Campbell, H. G. Flynn, D. T. Blackstock, C. Linke, and E. L. Carstensen, "The acoustic fields of the Wolf electrohydraulic lithotripter," J. Lithotripsy Stone Dis. **3**, 147–156 (1991).
[62]M. A. Beckett and I. Hua, "Impact of ultrasonic frequency on aqueous sonoluminescence and sonochemistry," J. Phys. Chem. A **105**, 3796–3802 (2001).
[63]A. M. L. Vinçotte, "A frequency study of sonoluminescence and sonochemical activity," MPhil thesis, University of Southampton, 1999.